NOTES AND CORRESPONDENCE

Dual-Polarization Radar Characteristics of an Apartment Fire

THOMAS A. JONES AND SUNDAR A. CHRISTOPHER

Department of Atmospheric Science, University of Alabama in Huntsville, Huntsville, Alabama

WALT PETERSEN

NASA Marshall Space Flight Center, Huntsville, Alabama

(Manuscript received 3 February 2009, in final form 27 May 2009)

ABSTRACT

Dual-polarimetric microwave wavelength radar observations of an apartment fire in Huntsville, Alabama, on 3 March 2008 are examined to determine the radar-observable properties of ash and fire debris lofted into the atmosphere. Dual-polarimetric observations are collected at close range (<20 km) by the 5-cm (C band) Advanced Radar for Meteorological and Operational Research (ARMOR) radar operated by the University of Alabama in Huntsville. Precipitation radars, such as ARMOR, are not sensitive to aerosol-sized ($D < 10\ \mu$m) smoke particles, but they are sensitive to the larger ash and burnt debris embedded within the smoke plume. The authors also assess if turbulent eddies caused by the heat of the fire cause Bragg scattering to occur at the 5-cm wavelength.

In this example, the mean reflectivity within the debris plume from the 1.3° elevation scan was 9.0 dBZ, with a few values exceeding 20 dBZ. The plume is present more than 20 km downstream of the fire, with debris lofted at least 1 km above ground level into the atmosphere. Velocities up to 20 m s^{-1} are present within the plume, indicating that the travel time for the debris from its source to the maximum range of detection is less than 20 min. Dual-polarization observations show that backscattered radiation is dominated by nonspherical, large, oblate targets as indicated by nonzero differential reflectivity values (mean = 1.7 dB) and low correlation coefficients (0.49). Boundary layer convective rolls are also observed that have very low reflectivity values (−6.0 dBZ); however, differential reflectivity is much larger (3.2 dB). This is likely the result of noise, because ARMOR differential reflectivity is not reliable for reflectivity values <0 dBZ. Also, copolar correlation is even lower compared to the debris plume (0.42). The remainder of the data mainly consists of atmospheric and ground-clutter noise. The large differential phase values coupled with positive differential reflectivity strongly indicate that the source of much of the return from the debris plume is particle scattering. However, given the significant degree of noise present, a substantial contribution from Bragg scattering cannot be entirely ruled out.

1. Introduction

The impacts of smoke on the environment have been well documented (e.g., Wang et al. 2006; Kahn et al. 2007). Large fires can inject substantial amounts (>1 Tg) of aerosol-sized particles ($D < 10\ \mu$m) into the atmosphere, which then have significant impacts on both nearby and downstream atmospheric conditions (Wang et al. 2006). Nearer to the fire, particles consisting of ash and partially burnt debris are also lofted into the atmosphere by the extreme localized buoyancy produced by the heat of the fire (Rothermel 1991; Banta et al. 1992). These particles, whose sizes may exceed several millimeters, generally fall out of the smoke plume within minutes to an hour as buoyant parcels become mixed with the surrounding atmosphere. However, the temporary presence of these larger particles may allow future research to assess smoke plume characteristics when measurements of the aerosols themselves are not available.

Several satellite-, surface-, and aircraft-based sensors exist today that can provide information on the columnar

Corresponding author address: Thomas A. Jones, Department of Atmospheric Science, University of Alabama in Huntsville, 320 Sparkman Drive, Huntsville, AL 35805.
E-mail: tjones@nsstc.uah.edu

DOI: 10.1175/2009JTECHA1290.1

aerosol optical depth of smoke aerosols, including the Moderate Resolution Imaging Spectroradiometer (MODIS), Multiangle Imaging SpectroRadiometer (MISR), Cloud-Aerosol Lidar and Infrared Pathfinder Satellite Observation (CALIPSO), and Aerosol Robotic Network (AERONET). These sensors can provide total column and in some cases vertical profile information on the aerosols being observed (e.g., CALIPSO). However, MODIS, MISR, and CALIPSO are all located onboard polar-orbiting satellites providing sampling once per day (MODIS) up to once per week or more (MISR and CALIPSO) for any single location. Surface AERONET measurement sites have high temporal resolution ($\leq$1 h), but they must be located very near the fire to be able to estimate its characteristics. Direct sampling of individual smoke plumes does exist in the form of aircraft measurements made as part of various field campaigns, such as the Arctic Research of the Composition of the Troposphere from Aircraft and Satellites (ARCTAS; Jacob et al. 2007) and FireFlux, which analyzed the changes in atmospheric conditions associated with controlled burns of grass fires (Clements et al. 2007). However, few in situ measurements of particle size, shape, and number concentration associated with the larger burnt biomass debris (BBD) near a fire's origin currently exist.

One currently underutilized tool for sampling smoke plume characteristics is radar (Rogers and Brown 1997). For intense fires, concentrations and sizes of particulate matter lofted into the atmosphere are sufficient to be detected by precipitation radars (PRs), such as the Weather Surveillance Radar-1988 Doppler (WSR-88D) network in the United States (Crum and Alberty 1993; Melnikov et al. 2008). These data provide the opportunity for both high-spatial- and high-temporal-resolution observations of fire events in near–real time. However, we must emphasize that precipitation radars are not sensitive to the aerosols themselves, but rather they are sensitive to larger millimeter-sized ash and debris particles lofted into the atmosphere. Longer wavelength (>10 cm) radars and profilers are also sensitive to backscattered radiation caused by large gradients in the refractive index on a scale less than one-half the radar wavelength, a phenomenon known as Bragg scattering (Doviak and Zrnic 1993). This phenomenon occurs in the presence of strong small-scale humidity and temperature gradients, which are also associated with large wildfires (Atlas 1960; Rogers and Brown 1997).

Before radar-derived debris plume characteristics can be assessed, we must first determine what the radar is actually observing. Several investigators have suggested the radar reflectivity from debris plumes is primarily due to scattering by large particle matter, such as ash, and partially burnt biomass, such as grass and pine needles, but with some disagreement on the importance of Bragg scattering relative to particle scattering (Banta et al. 1992; Rogers and Brown 1997; Erkelens et al. 2001). Two methods exist to solve this problem. The first is to use measurements of an individual debris plume at two different wavelengths to derive the difference in reflectivity. Rogers and Brown (1997) employed this method using a 3-cm radar and 33-cm profiler and concluded that Bragg scattering occurs at 33 cm but was not necessarily dominant. However, direct comparisons with 5- or 10-cm precipitation radars were not made. Because Bragg scattering is increasingly unlikely for smaller radar wavelengths (Rogers and Brown 1997; Erkelens et al. 2001), it seems likely that particle scattering dominates here.

Another method to distinguish between particle and Bragg scattering is the use of dual-polarimetric radar observations. Polarimetric radars are sensitive to the horizontally and vertically polarized radiation returned by the target objects with a preferred orientation, with the relative magnitude of horizontally versus vertically polarized reflectivity being a measure of particle shape (Bringi and Chandrasekar 2001). For nonspherically oriented particles, such as ash and pine needles, large differences should be readily apparent. Conversely, idealized spherical particles, such as small water drops ($D < 1$ mm), would be relatively polarization insensitive. Bragg scattering is also polarization insensitive; thus, it should be possible to determine the importance of Bragg scattering to returned reflectivity if polarimetric observations of a debris plume are available (Mueller and Larkin 1985).

We use the 5-cm Advanced Radar for Meteorological and Operational Research (ARMOR) Doppler radar observations of an ash and debris plume produced by an apartment fire in Huntsville, Alabama, to examine the question of particle versus Bragg scattering and describe the unique characteristics of debris plumes observed from radar. ARMOR is located less than 5 km away from the location of the fire providing the opportunity for very high-resolution polarimetric observations. The apartment fire itself lasted approximately 1 h between 1900 and 2000 UTC 3 March 2008. The fire, fueled by strong winds near the surface, destroyed several apartment units within the apartment complex and lofted substantial amounts of smoke and debris into the atmosphere. Radar observations of this debris are used as the basis to promote better understanding of characteristics of fires through analysis of the reflectivity, velocity, and polarimetric properties of the corresponding debris plume. The polarization characteristics of the debris plume are compared with those of other boundary layer

features present near the radar to determine the polarimetric properties of a debris plume that are unique to debris plume. While doing this, we also keep in mind the effects of radar noise and the multiple scattering mechanisms between the various targets on the interpretation of these differences. Once the question of what the radar is observing has been answered, it will then be possible for future research to correlate the radar observations with smoke plume characteristics to explore the effects of the downstream air quality of these fires.

2. Theoretical background

Before we can analyze Doppler radar–derived debris plume characteristics, we must first consider what exactly within the debris plume the radar actually detects. Precipitation radars send out a pulse of energy in the microwave spectrum, which is scattered back to a radar receiver by distributed scatters in the atmosphere. For a 5-cm radar, most precipitation targets (100 μm $< D <$ 1 cm), such as raindrops and snowflakes, are sufficiently small in size, which is explained by the Rayleigh approximation ($D < \lambda/16$) of Mie's solution to Maxwell's equations for the scattering of electromagnetic radiation by spherical particles. Under the Rayleigh regime, the backscattering cross section is proportional to the sixth power of the effective diameter of an individual spherical target D_i, as shown in the following equation, where K^2 is the dielectric constant and represents the contribution by the complex index of refraction for the particles being sampled:

$$\sigma_i = \frac{\pi^5 |K|^2 D_i^6}{\lambda^4}. \quad (1)$$

Because returned energy is a function of diameter to the sixth power, reflectivity values are highly sensitive to the largest particles in a particular volume. Because the relationship between the concentration, size, and composition of a particle to the magnitude of the returned energy is very nonlinear, reflectivity is generally reported in terms of effective reflectivity factor for water Z_e, which is expressed in decibel units (dBZ) and given by Eq. (2). Targets are assumed to be evenly distributed as spheres and to possess the dielectric constant of liquid water:

$$Z_e = 10 \log_{10}(z). \quad (2)$$

For larger particles, such as hail, where diameter and radar wavelength are similar, the Rayleigh approximation is no longer valid and the more complex Mie solution for spherical particles to Maxwell's equations must be considered (Rinehart 2004). Smaller wavelength radars ($\lambda \leq 3$ cm) are more sensitive to scattering in the Mie regime, as 3 cm radiation is closer in wavelength to large water droplets and hail than is 10 cm radiation. Further complications are introduced when particles such as large, bun shaped raindrops, become increasingly nonspherical violating both Rayleigh and Mie solutions. In this case, backscattering efficiency associated with nonspherical particles can differ significantly to that for spherical particles, complicating the interpretation of radar reflectivity values (Battan 1973).

The complex index of refraction and other parameters used to derive reflectivity use the assumption that microwave radiation is being scattered by liquid water drops; thus, reflectivity is actually water-equivalent reflectivity. For water droplets, $K^2 = 0.93$, whereas the value for ice is much lower (0.2; Rinehart 2004). Adams et al. (1996) derived a K^2 value of ~0.39 for dry, ash-like particles from biomass burning and volcanic emissions. Substituting the dry ash value into Eqs. (1) and (2) results in a reduction in apparent reflectivity by approximately 4 dB for the same particle size distributions. As a result, precipitation radars are somewhat less sensitive to ash and lofted fire debris compared to similarly sized water drops. Although it would be possible to replace these assumptions with those more appropriate for biomass burning while converting returned power to reflectivity, the resulting reflectivity values would not be comparable to anything in previous literature. It is also likely that these assumptions would vary significantly as a function of the type of biomass being burned and even the intensity of the fire. Thus, the remainder of this research defines ARMOR "reflectivity" as water-equivalent effective reflectivity Z_e. In this way, we may compare values with those previously reported in the literature and perform further analysis by using currently available processing algorithms.

Doppler radars can also be used to sample the velocity characteristics of debris plumes and the surrounding air mass. The faster a particle is moving relative to the radar, the greater the phase shift and the greater the radial velocity (Doviak and Zrnic 1993). A combination of reflectivity and velocity data are used here to estimate how far downwind of the apartment fire debris particles detectable by the radar remain suspended in the atmosphere.

Precipitation radars have been shown to be sensitive to many objects in addition to precipitation, including birds, insects, and—most importantly for this research—lofted matter from biomass burning (e.g., Doviak and Zrnic 1993). These radars are generally not sensitive to the smoke aerosols themselves, which generally have

diameters less than 10 μm. Using smoke aerosol particle distributions derived from Jayaratne and Verma (2001) and Hand et al. (2005) results in a smoke aerosol reflectivity Z_s of approximately -66 dBZ, using Eq. (3). Here, D_i ranges from 0 to 2 μm and a total $N_i \approx 10^{10}$ m^{-3}, where i represents one of several observed number density–particle size distributions N_i:

$$Z_s = 10 \log_{10}\left(\sum N_i D_i^6\right). \quad (3)$$

This value is well below the sensitivity of ARMOR at the range of interest (Table 1). It is clearly evident that the radar is not observing the smoke aerosols themselves.

Substantial amounts of atmospheric turbulence are also present in the vicinity of large fires, which is a result of the exchange of heat from the fire into the much cooler atmosphere above (Clements et al. 2007). This turbulence produces large gradients in temperature and humidity, which in turn results in gradients in the atmospheric index of refraction. If these gradients are on the order of one-half the wavelength of the radar or smaller, they will scatter radiation back to the radar, a phenomenon known as Bragg scattering. Because Bragg scattering is dependent on the length scale of the gradients relative to the radar wavelength, short wavelength radars ($\sim$3 cm) are less sensitive compared to longer wavelength radars, such as a 10-cm WSR-88D. Bragg scattering is not significant when reflectivity from two different wavelength radars is similar, assuming attenuation and noise are not factors. When Bragg scattering is important, large differences should be apparent for different wavelength observations. The relationship between Bragg scattering and reflectivity is expressed in the following, where C_n^2 is the refractive index structure constant, which depends primarily on gradients in the temperature and especially moisture fields (Knight and Miller 1993):

$$Z_b = \frac{0.38\lambda^{11/3}}{\pi^5 |K|^2} C_n^2. \quad (4)$$

Knight and Miller (1993) observed that, for large values of C_n^2 (3×10^{-11} m$^{-2/3}$), reflectivity from Bragg scattering Z_b was only $\sim$10 dBZ. This calculation assumes the use of the complex index of refraction of water droplets (0.93). This assumption remains, even though Bragg scattering is not sensitive to the water droplets themselves (Knight and Miller 1993). Substituting the value for ash (0.39) results in a somewhat higher Bragg scattering reflectivity value, indicating biomass-burning signatures may be more susceptible to Bragg scattering than those produced in a water cloud environment, but this assumption remains untested.

TABLE 1. ARMOR specifications and operating characteristics on 3 Mar 2008 (derived from Petersen et al. 2007).

Location	HSV
	34.65°N, 86.77°W
Transmit frequency	5625 MHz
Peak power	350 kW
Pulse width	0.8 μs
PRF	1200 Hz
Antenna diameter	3.7 m
First side lobe	<-28 dB
Minimum reflectivity -41 dBZ at range of 1 km	
Beamwidth	1.07°
Elevations	0.7°, 1.3°, 2.0°
Volume scan frequency	$\sim$1 scan per 5 min
Signal processor	Sigmet RVP8
Variables	Z, V_r, Z_{DR}, Φ_{DP}, K_{DP}, ρ_{hv}

Although the apartment fire was observed by both the 5-cm ARMOR and a 10-cm WSR-88D 65 km away (KHTX), the significant differences in sampling due to the difference in range from fire and scanning strategies make quantitative comparisons between the two impractical. Fortunately, it is also possible to distinguish particle from Bragg scattering using polarimetric radar observations (Mueller and Larkin 1985; Wilson et al. 1994). Particles produced from biomass burning, such as ash and other partially burnt debris, come in all shapes and sizes, in stark contrast to the relativity uniform spherical water drops found in light to moderate rainfall (e.g., Banta et al. 1992). Bragg scattering, on the other hand, is not polarization sensitive and should return the same reflectivity for both horizontally and vertically polarized radiation as long as it is not contaminated by noise (Mueller and Larkin 1985; Wilson et al. 1994). Thus, if scattering from nonspherical debris particles is the primary source of the radar fire signature, then the expected difference in horizontally versus vertically polarized reflectivity should be large. Conversely, if Bragg scattering is dominant, then this difference is small, assuming reflectivity is high enough to limit the impact of noise on the reflectivity at both polarizations. The relative difference in reflectivity between the two polarizations is typically expressed as a log ratio and termed the differential reflectivity, or Z_{DR}. Mathematically, Z_{DR} is expressed as

$$Z_{DR} = 10 \log_{10}\left(\frac{Z_h}{Z_v}\right). \quad (5)$$

Other polarimetric parameters measured by ARMOR include copolar correlation coefficient ρ_{hv} and differential phase Φ_{DP}. The copolar correlation is simply the correlation between samples of horizontally and vertically

polarized radiation at zero time lag, whereas differential phase Φ_{DP} represents a range-integrated phase shift Φ (in degrees) associated with differential forward scattering phase functions between the horizontal pulse k_h and vertical pulse k_v as the pulses move along the propagation path r, with Φ_{DS} being the differential phase upon scattering:

$$\Phi_{DP} = 2\int_0^{r_o} [k_h(r) - k_v(r)]\, dr + \Phi_{DS}. \qquad (6)$$

This parameter is sensitive to the shape, number concentration, and dielectric strength of the particles being observed. For example, a large number of oblate raindrops will increase Φ_{DP} with range resulting from the enhanced refraction, because horizontally polarized radiation progresses through the medium at a slower speed compared to the vertically polarized radiation. Specific differential phase K_{DP}, the range derivative of Φ_{DP}, is typically the variable used to detect regions of strong phase shift available, but in this study K_{DP} as computed by the current processing algorithm did not show any useful signal relating to the debris plume or boundary layer features; thus, it was not used in the analysis. Further discussion of polarimetric variables can be found in Bringi and Chandrasekar (2001). Ash and debris from the fire exhibits a unique signature in polarimetric space compared to Bragg scattering, raindrops, or other clear-air phenomena, and these distinctions are examined below.

3. Data

ARMOR is a scanning dual-polarimetric, 5-cm Doppler radar with a 1.07° azimuthal beamwidth that is currently operated by the University of Alabama in Huntsville (Petersen et al. 2007). ARMOR is located at the Huntsville International Airport (HSV), which is located less than 5 km southwest of the apartment complex. For this study, the debris plume is examined using data collected by ARMOR's "RAIN1" scan mode. During the RAIN1 scan, ARMOR operates in simultaneous transmit and receive mode (slant 45), at a range-gate spacing of 250 m, a pulse repetition frequency (PRF) of 1200 Hz, and at 64 horizontal and vertical samples per range bin. During the RAIN1 scan, ARMOR completes three full sweeps at elevation angles of 0.3°, 1.7°, and 2.0° (Table 1).

The ARMOR radar is calibrated as a system on a regular basis using built-in receiver calibration software, noise sources, solar scans, vertically pointing (90° elevation angle) data collections in light precipitation (absolute calibration of Z_{DR}), and internal consistency checks among the polarimetric variables (i.e., K_{DP}, Z_e, and Z_{DR}) after attenuation/differential attenuation corrections are completed (Bringi et al. 2006). The attenuation correction algorithm is automatically called regardless of the presence of precipitation. If there is no precipitation in the volume, then the only attenuation correction completed is done in the radar processor via standard range-based corrections applied for gaseous attenuation (Doviak and Zrnic 1993). Consistency checks on the overall "health" of the ARMOR system are also conducted in weather via examination of ρ_{hv} performance in light precipitation and drizzle ($22 < Z_e < 25$ dBZ), where the value of ρ_{hv} should be 0.99 or greater and Z_{DR} tends to be near 0 dB. Typically, ARMOR measures ρ_{hv} values >0.99 in drizzle and light rain and Z_{DR} biases remain relatively stable at $+0.5 \pm 0.75$ dB, with an overall Z_{DR} error of ± 0.25 dB. The variation of the differential phase along individual rays in the same precipitation situations is typically less than 3°.

In addition to active, near-real-time calibration activities, post analysis and comparison of the data for specific events provide another way of calibrating the radar—especially reflectivity. For example, it was discovered for days just prior to and after the fire event that ARMOR's reflectivity was biased approximately 2 dB low relative to the Tropical Rainfall Measurement Mission (TRMM) satellite PR. Because the TRMM PR is assumed to possess a relatively stable calibration, a significant deviation (e.g., more than 1–1.5 dB) of ARMOR reflectivity values from those of the TRMM-PR is assumed to indicate a drift in the calibration of ARMOR. Indeed, postanalysis internal consistency checks for cases that occurred on 26 February 2008 and 4 March 2008 suggested that ARMOR possessed a bias in reflectivity of −2 dB. Examination of the radar logs indicated that a receiver calibration was missed in late February 2008. Upon completion of a receiver calibration on 13 March 2008, prior to the next rain event on 14 March 2008, postanalysis of data indicated that the bias was removed. Despite the bias, we remain confident that both the dual-polarimetric and reflectivity variables used for this particular case study are providing important observations. To account for this bias, reported values for ARMOR reflectivity were adjusted 2 dB upward for the remainder of this research. Data from the volume scan starting at 1930 UTC are examined, which represents the time when the fire was near its peak intensity.

4. Noise and clutter

Another important consideration is the effect of ground clutter and radar signal-to-noise ratio (SNR) on the interpretation of the polarimetric results. For example,

anomalously low ρ_{hv} coupled with anomalously high values of Z_{DR} are often an indicator of low SNR values, especially when reflectivity is low (<10 dBZ). All of these conditions are present in our apartment fire observations; thus, great care is required in separating the noise from the signal. Because the ARMOR observations of the fire are collected near the radar and possess relatively low reflectivities, ground clutter also poses a significant problem in the interpretation of the polarimetric variables. As a result, certain efforts to mitigate the effects of noise sources on the output variables must be made. To more clearly delineate the polarimetric smoke signatures from the background, several thresholds are applied to the raw data prior to the analysis described in section 5. Reflectivity values greater than 40 dBZ are removed, because inspection indicated that these large values at close range are associated with ground-clutter artifacts. For the same reason, data where the radial velocity is less than ± 1 m s^{-1} were also removed. Differential reflectivity values in excess of ± 8 dB exceed the span of those recorded by the radar processor in its current setup configuration and are removed by default. Finally, the copolar correlation is also constrained to be >0.1, though this threshold only removes a few percent of the total number of data points. Larger values for ρ_{hv} thresholds are not used, because the debris particles themselves are expected to have values <0.5. Finally, only data within 40 km of the radar are analyzed. Despite these thresholds, significant noise remains, especially at the lowest elevation scan (0.7°) within 15 km of the radar. As a result, data associated with the debris plume and convective rolls are manually partitioned from the background by using human interpretation. Some uncertainty exists in this separation, and only the convective roll features to the east of the radar are separated from the remainder of the data. Uncertainty in the debris plume is greatest within 15 km of the radar, especially for low-reflectivity pixels.

5. Analysis

a. Reflectivity

We examine the hypothesis that particle scattering is dominant in precipitation radar observations of fire events by analyzing their reflectivity, velocity, and polarimetric characteristics relative to theory and surrounding boundary layer characteristics. Figures 1a–c shows ARMOR reflectivity at ~1930 UTC at 0.7°, 1.3°, and 2.0° elevations, after the initial data filtering previously described. The debris plume originating from the apartment fire is clearly visible along with other boundary layer features arranged in a south–north direction east of the fire. The fire extends from the apartment complex northward, being visible from ARMOR at ~20 km downwind of its origin. It remains evident at the 2.0° elevation at this range, indicating that the debris has reached a height of at least 1 km above the surface. Debris could be present even higher in the atmosphere, but higher elevation scans are not present to accurately determine the maximum altitude where the debris is present. The debris plume is visible from ARMOR for almost an hour between 1900 and 2000 UTC; during that time, portions of the debris plume extend up to 30 km away from the fire. This occurs after 1930 UTC, when reflectivity near the fire itself is already decreasing.

The amount of debris lofted into the air by this fire is so great that was observable from the (KHTX, Hytop) WSR-88D radar approximately 65 km away, around 1930 UTC (Fig. 2). At this range, the WSR-88D has a much lower sampling resolution than ARMOR; it would be reasonable to expect that reflectivity from the WSR-88D would be lower. However, the WSR-88D also observed reflectivity >20 dBZ and had an average reflectivity nearly 3 dB greater than ARMOR. The opposite would be expected if Rayleigh particle scattering was the largest contributor to reflectivity; thus, neither Bragg nor nonspherical particle scattering can be ruled out at this stage. The combined differences in radar characteristics, calibration procedures, scanning strategies, and the range of the observations limit the possibility of any further quantitative assessment of the differences between ARMOR and WSR-88D observations.

Approximately 70% of ARMOR reflectivity values (adjusted to correct for the 2-dB bias) range between −3 and 18 dBZ, with a few pixels exceeding 20 dBZ (Fig. 2a). Histograms for this and other parameters use data from the 1.3° elevation. Distributions from other elevations are similar (not shown). Mean reflectivity is 9.0 dBZ, which would correspond to nonprecipitating clouds or possibility very light drizzle if liquid water drops are being observed. Along the edges of the debris plume, reflectivity is less than 0 dBZ as the debris disperses laterally in the atmosphere. Reflectivity decreases (as does noise) somewhat with height, because the larger, heavier debris particles are likely located nearer to the surface (Figs. 1a–c).

Although the debris plume is clearly evident from the reflectivity data, other features are also present. Lines of weak reflectivity (≤ -5 dBZ) are present along a south–north orientation parallel to that of the mean wind direction. These features are a representation of convective turbulence in the boundary layer resulting from variations in surface heating that produce convective rolls (e.g., Doviak and Zrnic 1993). Lines of boundary cumulus are also evident from MODIS visible

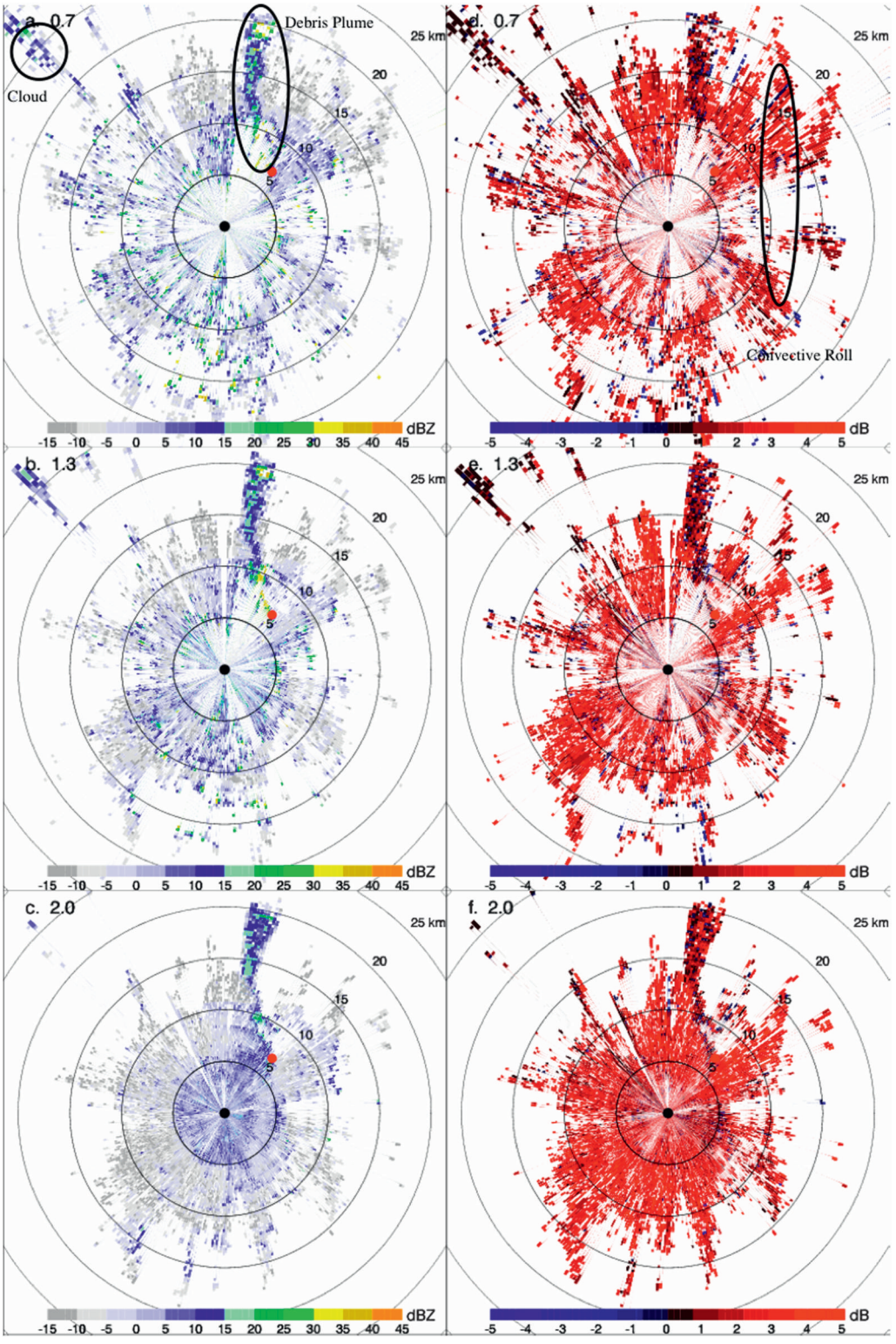

FIG. 1. (a)–(c) Reflectivity (dBZ) and (d)–(f) Z_{DR} (dB) for 0.7°, 1.3°, and 2.0° elevation scans at approximately 1930 UTC 3 Mar 2008 from the ARMOR radar located at HSV. Gray circles indicate 5-km range rings and the red circle indicates the location of the apartment complex. Fire, convective rolls, and cloud features are denoted.

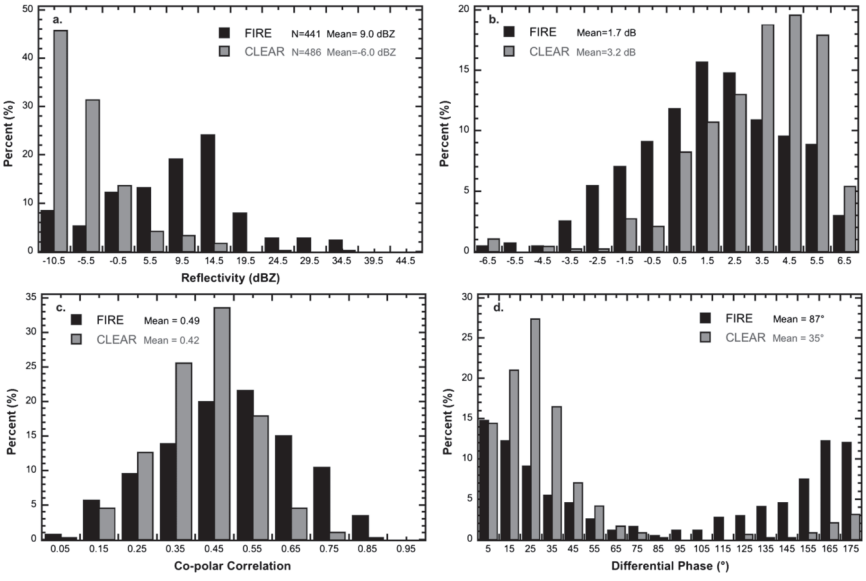

FIG. 2. Histograms of (a) reflectivity, (b) Z_{DR}, (c) ρ_{hv}, and (d) Φ_{DP} for ARMOR data associated with the fire debris plume (black) and data associated with the boundary layer convective rolls (gray).

satellite image at this time (Fig. 3). The strongest linear features lie well east of the radar (>40 km) and decrease in strength westward toward the radar. (Unfortunately, upper-level cirrus is obscuring the lower-level smoke plume from the satellite). Convective rolls can be detected through the gradients in temperature and moisture they produce, increasing the value of C_n^2 (i.e., Bragg scatter) and/or particles (or insects) uplifted into the convective roll by gusty winds near the surface (Doviak and Zrnic 1993). Reflectivity associated with these features are generally very low, with a mean value of −6.0 dBZ associated with those east of the radar (Fig. 1a).

Interestingly, the debris plume lies along the line where the convective boundary would be if the fire was not present, assuming the distance between convective rolls was constant. The localized increase in buoyancy along the convective roll may be allowing for farther and higher transport of fire debris than would otherwise be the case, though no conclusive evidence exists that this is actually occurring. Finally, there is the noise that is evident within 15 km of the radar location. Within this noise area, no particular pattern in the data exists, except a slight decrease in reflectivity as a function of range and elevation, indicating the presence of ground clutter (Fig. 1). This noise accounts for approximately 85% of the pixels that pass through the filtering described in section 4. One additional feature is present, which is characterized by a small area of 5–15-dBZ values 25 km northwest of the radar. Based on satellite imagery, this appears to be a small area of cumulus congestus (Fig. 3). Concrete distinctions between actual atmospheric phenomena and noise must be made before the scattering characteristics of the debris plume can be resolved with any degree of certainty.

b. Polarimetric parameters

The distinction between Bragg scatter and particle scattering can also be determined by using polarimetric observations. Recall that Bragg scatter does not favor horizontally or vertically polarized radiation. Thus, $Z_{DR} \approx 0$ when Bragg scattering is dominant (Wilson et al. 1994). Conversely, if nonspherical particle scattering is dominant, then the absolute value of Z_{DR} will be nonzero. Ash and fire debris associated with an apartment fire are likely very nonspherical in nature and will favor one polarization over the other. Figure 2b shows that Z_{DR} associated with the debris plume is decidedly nonzero, with a mean value of 1.7 dB at 1.3°. If data where reflectivity <10 dBZ are removed, then the mean Z_{DR} associated with the debris plume becomes 1.2 dB, indicating that some of the positive values associated with the weaker reflectivities may be impacted by noise. However, noise is less likely to be producing positive Z_{DR} values as reflectivity increases. The copolar correlation ρ_{hv} is also quite low (0.49), indicating a large variety of particle shapes and sizes being observed within each sample volume (Figs. 2c, 4e). Low values of ρ_{hv} can result from low signal-to-noise ratio, especially when reflectivity is low. Approximately 50% of Φ_{DP} observations associated with the fire plume have a

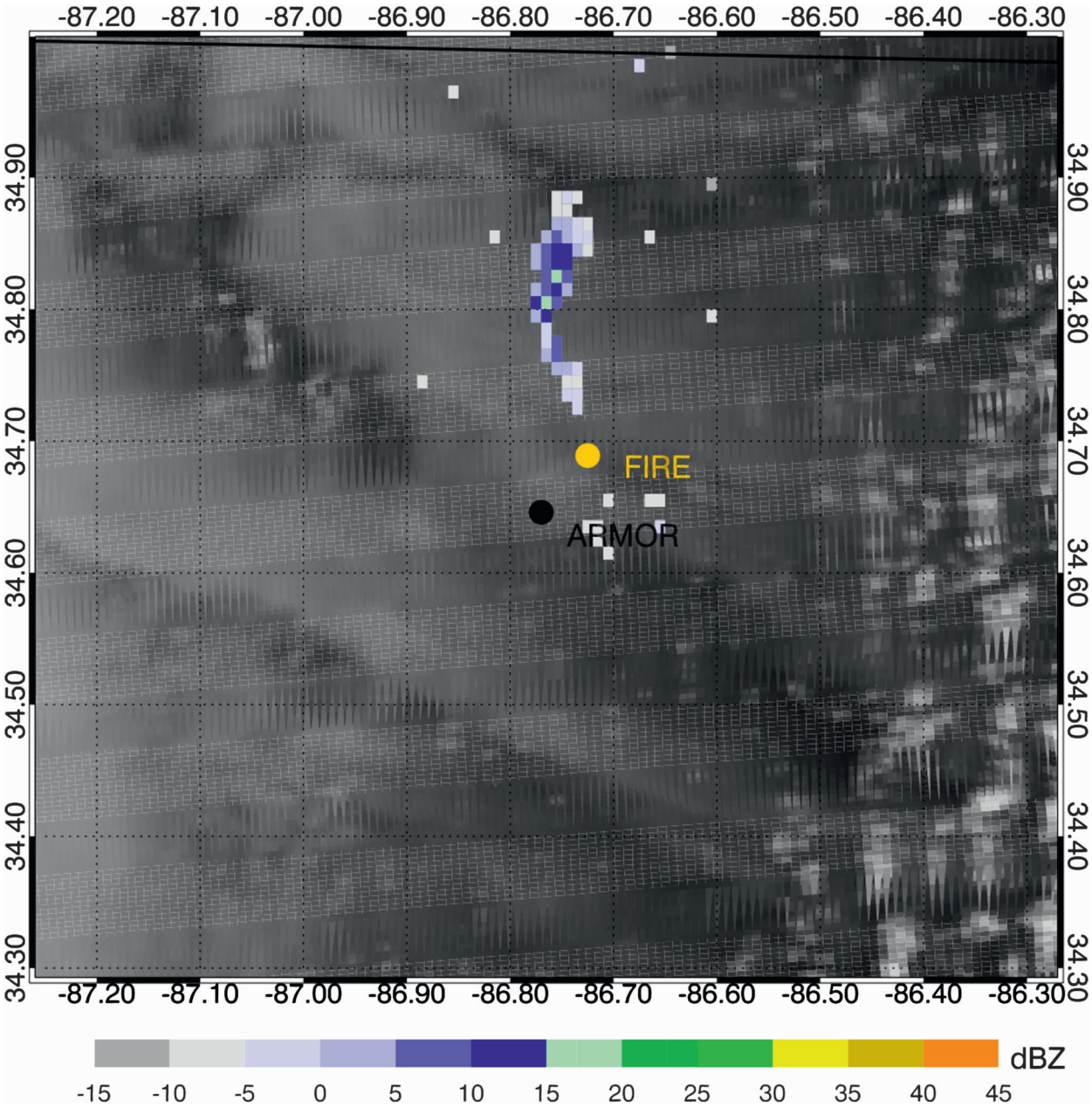

FIG. 3. MODIS visible image at 250-m resolution at 1935 UTC 3 Mar 2008. The locations of the ARMOR radar and the nearby apartment fire are given. Note that upper-level cirrus clouds are obscuring the smoke from the satellite's view; thus, reflectivity from the KHTX WSR-88D radar at 1938 UTC is given to indicate the position of the debris plume. KHTX is located approximately 65 km northeast of the fire, outside the domain of the figure. Another feature of interest is the convective rolls east of the radar aligned along a north–south axis and an isolated cloud feature approximately 25 km northwest of the radar. The linear bands oriented in an east–west pattern represent striping occurring in the data as a result of an issue with the MODIS instrument, but the atmospheric features of interest remain clearly visible.

differential phase greater than 90°, and the system phase is typically 11°–20°; however, the exact interpretation of the Φ_{DP} observations relative to the debris and low signal-to-noise environment remain unclear (Figs. 2d, 4b). Assuming these observations are a result of particle scattering, the positive Z_{DR} values observed within the debris plume indicate the presence of particles whose primary axis lies in the horizontal plane, similar to large raindrops ($D > 5$ mm). Ash from biomass burning and volcanic activity has been observed to have similar

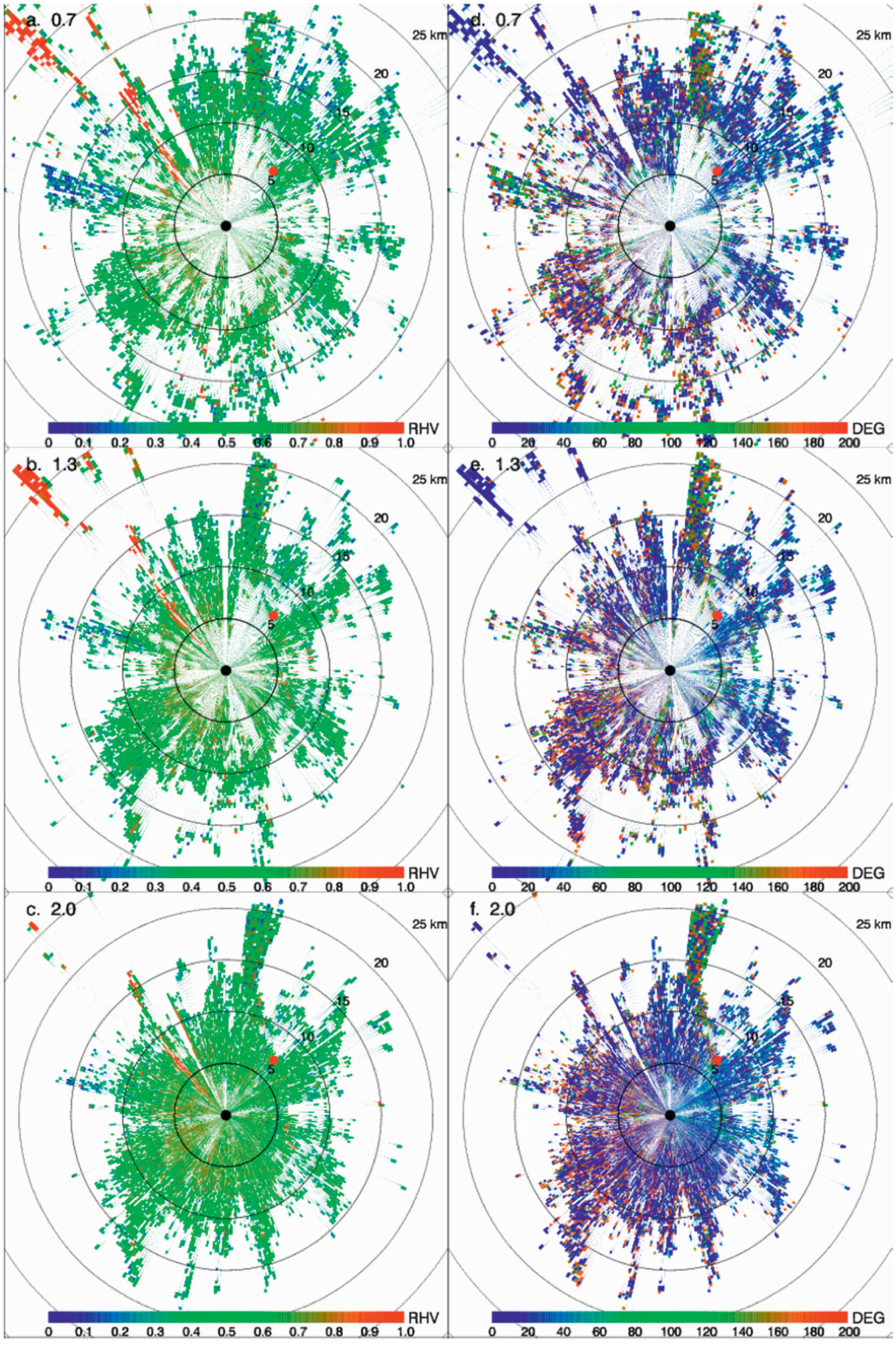

FIG. 4. As in Fig. 1, but for (a)–(c) ρ_{hv} and (d)–(f) Φ_{DP}. Note that data associated with the debris plume generally have much lower ρ_{hv} values than the cloud feature to the northwest.

shape characteristics (Banta et al. 1992). Similar results were obtained by Melnikov et al. (2008) using polarimetric observations of grass fires in central Oklahoma. It is also possible that the positive Z_{DR} values are a result of horizontally oriented needle-like particles (e.g., grass), but this seems unlikely given the nature of what is being burned. By comparison, observations of light to moderate rainfall would show Z_{DR} values near 0 dB and ρ_{hv} values near 1.0, because water droplets in this regime are primarily spherical and more evenly distributed.

No precipitation is present at the time of the apartment fire, but several boundary layer features and general noise are present. The distributions of Z_{DR} and ρ_{hv} between the debris plume and the boundary features do differ but not quite as expected. Copolar correlation associated with the convective rolls is actually lower (0.42) and Z_{DR} is higher (3.2 dB), whereas mean reflectivity is much lower, only –6.0 dBZ (Figs. 2a,b). Convective rolls are generally observed via the presence of insects caught up in the convergent portions of the rolls, generally resulting in weak values of reflectivity on the order of −10 to 0 dBZ for small insects (Gossard 1990; Wilson et al. 1994). Recall that the polarimetric values from ARMOR are increasingly unreliable at such low reflectivities. The noise apparent in the low-reflectivity data results in the rather high values of Z_{DR} observed. If pixels where reflectivity less than 0 dBZ are removed, then mean Z_{DR} decreases to 2.7 dB, indicating that noise has a greater impact when reflectivity is low, which is consistent with measurements from within the debris plume. However, only 10% of the data associated with the boundary layer features have $Z_e > 0$ dBZ.

The differential phase also provides a distinction between the debris plume and convective rolls. Here, 90% of Φ_{DP} values are less than 60°, with a mean value of only 35° compared to 87° within the debris plume. Similar low Φ_{DP}–high Z_{DR} values were observed in clear-air returns near the radar by Melnikov et al. (2008) and were attributed to insects and birds in the boundary layer. However, they reported ρ_{hv} values around 0.7 under these conditions, which is higher than that observed by this research (0.4). This indicates that either Alabama insects have different shapes than Oklahoma insects or more likely that the greater sensitivity of ARMOR compared to the WSR-88D results in the former being more susceptible to noise in clear-air conditions, resulting in the lower ρ_{hv} values. Scattering from water droplets with the boundary layer cumulus clouds also seems to be an unlikely source for the majority of the returned radiation, because ρ_{hv} should be near 1.0 if this was the case. Conversely, the polarimetric variables strongly indicate the presence of water droplets in the cloud observed northwest of the radar (Fig. 1b). Here, ρ_{hv} is >0.9 and Z_{DR} is near 0, indicating a relatively uniform distribution of spherical particles (Figs. 1e, 4e).

Despite the presence of noise, the polarimetric variables associated with the debris plume strongly indicate that some sort of particle scattering is occurring. However, noise and ground clutter may be influencing data, especially within 15 km of the radar. The large temperature gradients along the edge of the debris plume may be responsible for a portion of the returned radiation, because reflectivity along the edge is low (<−5 dBZ), but this is difficult to quantify. For comparison, data from a recent grass fire occurring on 16 February 2009 observed from ARMOR at a range of 40 km were compared with the apartment fire results. At this range, noise and ground clutter were less of an issue. The polarimetric properties of this grass fire are remarkably similar to those of the apartment fire and those presented by Melnikov et al. (2008). Given this observation, we feel that the polarimetric properties associated with the apartment fire described by this paper are not being heavily contaminated by noise.

c. *Radial velocity and debris lifetime*

Because the debris plume lies only a few degrees off the beam radial, velocity estimates of the debris particles are likely very close to their actual velocity, considering that the tangential component to the radar is small. Doppler velocity data from AMROR indicate that portions of the debris plume are traveling northward at an average speed of 15 m s^{-1}, with some values exceeding 20 m s^{-1} (Figs. 1a, 5). At this time, the surface station at the Huntsville Airport (the same location as the radar) reported a sustained surface (10 m) wind speed of 12 m s^{-1} with gusts of 16 m s^{-1} from 170° (from almost due south). These winds acted to increase the intensity of the fire and loft larger than normal debris downwind than would be the case in a weaker wind environment. Assuming most of the returned radiation is a result of ash and burnt debris particles, then particles large enough to be detected by the radar would fall out of the atmosphere within 20–30 min. Unfortunately, few actual observations of ash and/or debris plume particle distributions actually exist, which limits our ability to accurately derive some sort of debris number and size distribution within the plume based on radar data alone. Hopefully, future polarimetric observations can be made in situations where this distribution can be independently sampled.

6. Conclusions

Dual-polarization 5-cm radar observations of an apartment fire in Huntsville, Alabama, strongly suggest that

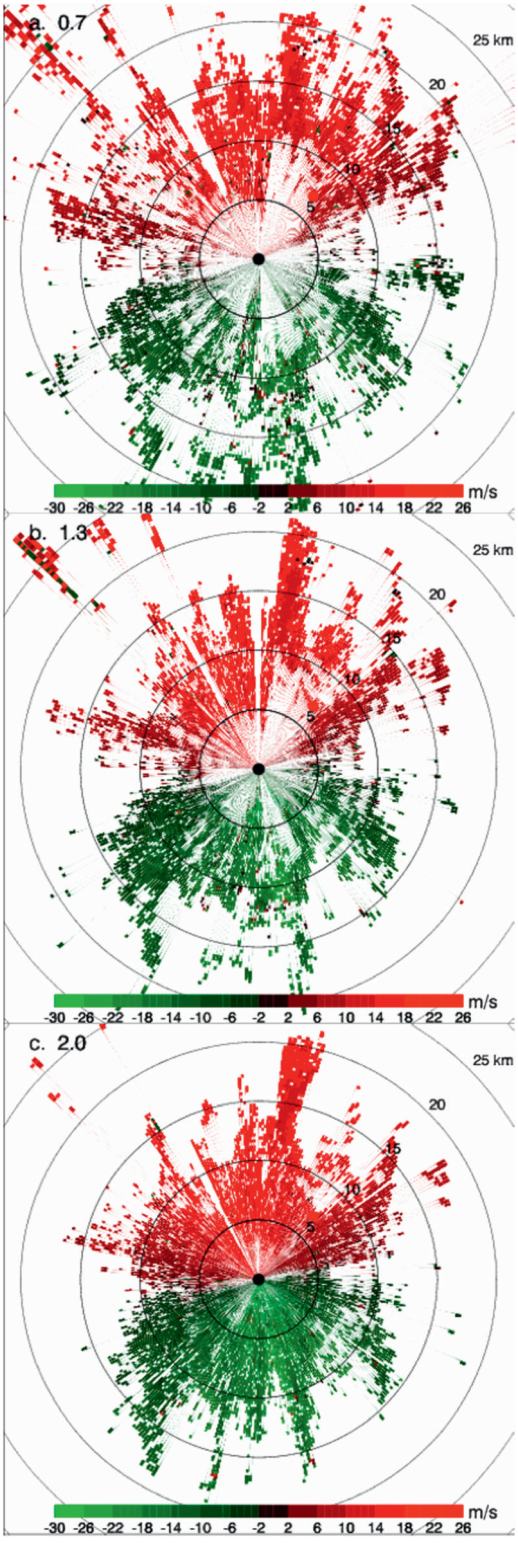

FIG. 5. Radial velocity (m s^{-1}) for (a) 0.7°, (b) 1.3°, and (c) 2.0° elevation scans. Winds are emanating from the south at between 15 and 20 m s^{-1} in the vicinity of the apartment fire.

particle scattering from large, millimeter-sized debris particles have unique polarimetric properties compared to cloud and other clear-air returns. ARMOR observations indicate that particle scattering (though not necessarily Rayleigh scattering) is more important relative to Bragg scatter, though it is possible that Bragg scattering is responsible for some of the weak reflectivity returns (<-5 dBZ) along the edges of the debris plume. Evidence for particle scattering exists in the positive but noisy Z_{DR} values within the debris plume. Positive Z_{DR} coupled with low ρ_{hv} values are indicators of highly nonspherical particles in the sample volume. The variability of particle number, size, and shape concentrations leads to low ρ_{hv} values and a "patchy" appearance of the radar data in this region. Weaker reflectivity values exist in association with boundary layer convective rolls that are present parallel to the mean wind flow (south–north). Interestingly, ρ_{hv} is lower and Z_{DR} is greater for these features compared to the debris plume. However, polarimetric parameters from ARMOR are not reliable for very low reflectivity values; thus, it appears that noise is adversely affecting the signal associated with the convective rolls. Additional noise in the form of ground-clutter contamination and possibly insects also exists within 15 km of the radar. However, the spatial uniformity of these parameters is greater for these clear-air features relative to the debris plume. Finally, a cumulus cloud northwest of the radar is associated with Z_{DR} near 0 dB and $\rho_{hv} > 0.9$, very consistent with large water droplets that would be expected in growing cumulus cloud.

The polarimetric characteristics associated with the apartment fire are remarkably similar to those presented by Melnikov et al. (2008) for a grass fire in Oklahoma using the KOUN WSR-88D and another grass fire recently observed from the ARMOR radar. Despite the differences in radar characteristics and apartment versus grass fires themselves, clear distinctions between the debris plume and other atmospheric phenomena are clearly evident. In both cases, debris plumes are characterized by modest reflectivity ($-10 < Z_e < 20$ dBZ), low copolar correlations ($\rho_{hv} < 0.5$), and consistently positive Z_{DR}. The greatest difference noted between this and the previous study was that Melnikov appeared to have higher ρ_{hv} values associated with noise and ground clutter. However, given the differences in noise filtering and ground-clutter suppression methods between the two radars, such a difference is not unexpected. Future research will incorporate additional case studies from grass and forest fires to compare the differences in the radar signatures as a function of the matter being burned. Radar observations of debris will be compared to in situ ash and smoke observations to produce a quantitative relationship between the properties of

aerosol-sized particles with those of the larger debris particles being observed by the radar. It should then be possible using the polarimetric data to create objective algorithms that can distinguish fire signatures from clouds and precipitation; work in this area is already underway (Melnikov et al. 2008; Jones and Christopher 2009).

Acknowledgments. This research was partially supported by NOAA Grants NA06NES4400008 and NA07NES4280005 and a NASA CALIPSO science team grant. MODIS data were obtained from the Level 1 and Atmosphere Archive and Distribution System (LAADS) at Goddard Space Flight Center (GSFC). Special thanks to Ms. Elise Johnson and Mr. Christopher Schultz for providing and formatting the ARMOR data used in this research and Ms. Christina Crowe of the Huntsville National Weather Service Office for providing the surface weather observations. We greatly appreciate the comments provided by the anonymous reviewers and the technical overview by Ms. Anita Leroy, which significantly improved the quality of this work.

REFERENCES

Adams, R. J., W. F. Perger, W. I. Rose, and A. Kostinski, 1996: Measurements of the complex dielectric constant of volcanic ash from 4 to 19 GHz. *J. Geophys. Res.,* **101,** 8175–8185.

Atlas, D., 1960: Radar detection of the sea breeze. *J. Meteor.,* **17,** 244–258.

Banta, R. M., L. D. Olivier, E. T. Holloway, R. A. Kropfli, B. W. Bartram, R. E. Cupp, and M. J. Post, 1992: Smoke-column observations from two forest fires using Doppler lidar and Doppler radar. *J. Appl. Meteor.,* **31,** 1328–1349.

Battan, L. J., 1973: *Radar Observation of the Atmosphere*. The University of Chicago Press, 324 pp.

Bringi, V. N., and V. Chandrasekar, 2001: *Polarimetric Doppler Weather Radar: Principles and Applications*. Cambridge University Press, 636 pp.

——, M. Thurai, K. Nakagawa, G. J. Huang, T. Kobayashi, A. Adachi, H. Hanado, and S. Sekizawa, 2006: Rainfall estimation from C-band polarimetric radar in Okinawa, Japan: Comparisons with 2D-video disdrometer and 400 MHz wind profiler. *J. Meteor. Soc. Japan,* **84,** 705–724.

Clements, C. B., and Coauthors, 2007: Observing the dynamics of wildland grass fires: FireFlux – A field validation study. *Bull. Amer. Meteor. Soc.,* **88,** 1369–1382.

Crum, T. D., and R. L. Alberty, 1993: The WSR-88D and the WSR-88D Operational Support Facility. *Bull. Amer. Meteor. Soc.,* **74,** 1669–1687.

Doviak, R. J., and D. S. Zrnic, 1993: *Doppler Radar and Weather Observations*. 2nd ed. Academic Press, 562 pp.

Erkelens, J. S., V. K. Venema, H. W. Russchenberg, L. P. Lightart, 2001: Coherent scattering of microwaves by particles: Evidence from clouds and smoke. *J. Atmos. Sci.,* **58,** 1091–1102.

Gossard, E. E., 1990: Radar research on the atmospheric boundary later. *Radar in Meteorology: A Collection of Essays in Honor of David Atlas, Meteor. Monogr.,* No. 52, Amer. Meteor. Soc., 477–527.

Hand, J. L., and Coauthors, 2005: Optical, physical, and chemical properties of tar balls observed during the Yosemite Aerosol Characterization Study. *J. Geophys. Res.,* **110,** D21210, doi:10.1029/2004JD005728.

Jacob, D. J., and Coauthors, 2007: Arctic research of the composition of the troposphere from aircraft and satellites (ARCTAS). NASA International IGAC/POLARCAT Experiment for the International Polar Year 2007-8 White Paper, 31 pp.

Jayaratne, E. R., and T. S. Verma, 2001: The impact of biomass burning on the environmental aerosol concentration of Gaborone, Botswana. *Atmos. Environ.,* **35,** 1821–1828.

Jones, T. A., and S. A. Christopher, 2009: Injection heights of biomass burning debris estimated from WSR-88D radar observations. *IEEE Trans. Geosci. Remote Sens.,* **47,** 2599–2605.

Kahn, R. A., W.-H. Li, C. Moroney, D. J. Diner, J. V. Martonchik, and E. Fishbein, 2007: Aerosol source plume physical characteristics from space-based multiangle imaging. *J. Geophys. Res.,* **112,** D11205, doi:10.1029/2006JD007647.

Knight, C. A., and L. J. Miller, 1993: First radar echoes from cumulus clouds. *Bull. Amer. Meteor. Soc.,* **74,** 179–188.

Melnikov, V. M., D. S. Zurnic, R. M. Rabin, and P. Zhang, 2008: Radar polarimetric signatures of fire Plumes in Oklahoma. *Geophys. Res. Lett.,* **35,** L14815, doi:10.1029/2008GL034311.

Mueller, E. A., and R. P. Larkin, 1985: Insects observed using dual-polarization radar. *J. Atmos. Oceanic Technol.,* **2,** 49–54.

Petersen, W. A., K. R. Knupp, D. J. Cecil, and J. R. Mecikalsi, 2007: The University of Alabama Huntsville THOR Center instrumentation: Research and operational collaboration. Preprints, *33rd Int. Conf. on Radar Meteorology,* Cairns, Australia, Amer. Meteor. Soc., 5.1. [Available online at http://ams.confex.com/ams/pdfpapers/123410.pdf.]

Rinehart, R. E., 2004: *Radar for Meteorologists*. 4th ed. Rinehart, 482 pp.

Rogers, R. R., and W. O. Brown, 1997: Radar observations of a major industrial fire. *Bull. Amer. Meteor. Soc.,* **78,** 803–814.

Rothermel, R. C., 1991: Predicting behavior and size of crown fires in the northern Rocky Mountains. U.S. Dept. of Agriculture, Forest Service, Intermountain Research Station, Research Paper INT-438, 46 pp.

Wang, J., S. A. Christopher, U. S. Nair, J. S. Reid, E. M. Prins, J. Szykman, and J. L. Hand, 2006: Mesoscale modeling of Central American smoke transport to the United States: 1. ''Top-down'' assessment of emission strength and diurnal variation impacts. *J. Geophys. Res.,* **111,** D05S17, doi:10.1029/2005JD006416.

Wilson, J. W., T. M. Weckworth, J. Vivekanandan, R. M. Wakimoto, and R. W. Russell, 1994: Boundary layer clear-air radar echoes: Origins of echoes and accuracy of derived winds. *J. Atmos. Oceanic Technol.,* **11,** 1184–1206.